Supporting Information

Gautam et al. 10.1073/pnas.1008240107

SI Text

Details on the Preparation of Unipolar Al-Doped Zinc Oxide (ZnO) Assemblies. In order to synthesize unipolar ZnO 1D assemblies, 600 mg of $Zn(CH_3COO)_2.2H_2O$ and 30 mg of $Al(NO_3)_3.9H_2O$ were used as Zn and Al precursors and NaOH (2.2 g) was used as the corresponding hydrolyzing agent. The precursors were dissolved in 40 mL mixed solvent of water and ethanol (1:1 volume ratio) by in ultrasonic water bath for 30 min and then transferred in to a Teflon-lined autoclave (filling fraction: 80%). The sealed autoclave was inserted into a hot-air oven that was preheated to 200 °C and kept at this temperature for 24 h before allowing it to cool naturally. After the reaction, the white products were washed with deionized water and ethanol and dried at 60 °C in vacuum for 24 h.

We found that under these synthesis conditions the presence of the Al is crucial for obtaining the concentric assemblies. When the reaction was carried out in the absence of the Al precursor, freestanding ZnO nanorods were obtained. However, it is also possible to obtain similar assemblies without using Al doping under certain conditions (1, 2). Also, similar structures are reported for other materials such as CdS and CdSe, having an identical crystal structure with ZnO (3).

The as-prepared product was characterized by using X-ray diffraction (SEIFERT, 3000TT with Cu Kα, $\lambda = 0.15418$ nm α-radiation), field-emission SEM (JSM-6700F), and a transmission electron microscope (TEM) (JEM-3000F), equipped with an energy-dispersive X-ray spectroscope (EDS). After the structural and chemical examinations, spatially resolved cathodoluminescence (CL) measurements on individual ZnO assemblies were carried out. CL spectra were collected with a high-resolution CL system employing accelerating voltages of 10 kV and at a constant current density of 2000 pA at room temperature, by using Ultra-High Vacuum SEM and a Gemini electron gun (Omicron) equipped with a CL system (4). The vacuum of the specimen chamber was maintained at 10^{-11} mbar.

Convergent Beam Electron Diffraction (CBED) Image Simulation. Simulated CBED patterns were obtained by many-beam dynamical calculations. The intensity calculation is based on the Bloch-wave formulation of dynamical theory (5). The basic parameters used were as follows:

$a = 3.249$, $b = 3.249$, $c = 5.207$
$\alpha = 90.00$, $\gamma = 120.00$
Space group P63mc (186)
$V_{acc} = 300$ kV
Incident beam plane $(10\bar{1}0)$
Position O (x,y,z)

- $x = 0.33333$, $y = 0.66667$, $z = 0.37500$

Position Zn (x,y,z)

- $x = 0.33333$, $y = 0.66667$, $z = 0.00000$

Estimation of Variation of Optical Properties Inside ZnO Assemblies. Cathodoluminescence images show that emission properties of rods gradually change from the tip of the rods to the base. All rods in one type of assembly show similar behavior, and therefore to estimate variations within the two assemblies, we systematically investigated different rods in the following manner: CL spectra were recorded along the rod from tip to the base in 10 equally spaced positions.

Fig. S5 shows two Zn-polar ZnO rods before and after CL investigation. Due to bombardment with the electron beam, the surface of the structure gets partially damaged (giving an idea of CL probe beam exposure area). Two adjacent probe areas are independent of each other. These assemblies provide a platform for investigating influence of growth direction on internal properties, because in freestanding ZnO rods, the growth would have taken place along either of the polar ends.

Simulation of Surface Roughness. The surface roughness of a growing crystal is defined as the standard deviation of the atom's position on the surface in the direction of the growth, measured in size of layers. And this, in a realistic scenario, will be attributed to various defects and dislocations, etc., on the surface. This, for a growing ZnO crystal, was simulated using Leocrystal software based on numerical Monte Carlo modeling (6). Fig. S7 shows a plot of surface roughness at different concentrations of reactants and surface energies. Roughness gradually decreases with the progress of a reaction because the concentrations of reactants decrease constantly. Roughness also depends on the surface energy, which in the case of Zn and the O-polar surfaces on a ZnO crystal are different. The growth behavior is identical for all rods in a single unipolar assembly and is suggested to have given rise to spatial luminescence patterns in these assemblies.

Parameters of Crystallization. ***Structure element.*** The lattice constants of hexagonal wurtzite zinc oxide are $a = 3.25$ Å and $c = 5.2$ Å with $n = 2$ in each cell, molar mass is 81.408 g/mol, and density is 5.606 g/cm^3. A technical requirement for this modeling is the description of the smallest crystal units as orthorhombic building blocks. The best approximation for the wurtzite ZnO parameters into orthorhombic symmetry can be achieved with one molecule in the lattice cell with parameters $a = 2.82$ Å, $b = 3.25$ Å, and $c = 5.2$ Å. Despite the change in the description of the building block, the variation of roughness would qualitatively remain same.

Thermodynamic parameters. The calculated melting temperature of pure ZnO is $T_a = 2221$ °C and enthalpy of crystallization $\Delta H = 35.2$ kJ/mol (7). The temperature of growth in accordance with synthesis procedure was set to 200 °C. The initial concentration of ZnO in 40 mL of water-ethanol (50:50) solution can be estimated using the following chain of reasons. The initial 0.6 g of Zn acetate is equivalent of 0.002733 mol or 0.222528 g ZnO. At the same time the weight of 40 mL of crystalline ZnO is 224 g. Hence the initial concentration of ZnO in solution is $0.222/224 = 0.001\%$ of pure ZnO. That leads to an initial equilibrium temperature of crystal growth equal to 219 °C.

For thermal frequency of molecules $\gamma_o = 2e^{14}$ s^{-1} (that is consistent to the sound rate in solid matter) and activation energy $E_a = 1.3e + 5$ J/mol that gives calculated growth rate for continuous mechanism estimated as 0.1 nm/s; i.e., with these values, about 10 h of growth can produce crystals with size 3.6 μm, which is in good agreement with experimental results. It is important to mention that the above values for thermal frequency and activation energy are rough estimations and are not supposed to be considered as measured experimentally.

1. Zhang R, Fan L, Fang Y, Yang S (2008) Electrochemical route to the preparation of highly dispersed composites of ZnO/carbon nanotubes with significantly enhanced electrochemiluminescence from ZnO. *J Mater Chem* 18:4964–4970.
2. Kim YJ, et al. (2008) Position-controlled ZnO nanoflower arrays grown on glass substrates for electron emitter application. *Nanotechnology* 19:315202.
3. Yao WT, et al. (2006) Architectural control syntheses of CdS and CdSe nanoflowers, branched nanowires, and nanotrees via a solvothermal approach in a mixed solution and their photocatalytic property. *J Phys Chem B* 110:11704–11710.
4. Yuan XL, Dierre B, Wang JB, Zhang BP, Sekiguchi TJ (2007) Spatial distribution of impurities in ZnO nanotubes characterized by cathodoluminescence. *J Nanosc Nanotech* 7:3323–3327.
5. Tsuda K, Tanaka M (1999) Refinement of crystal structural parameters using two-dimensional energy-filtered CBED patterns. *Acta Cryst A* 55:939–954.
6. Sakharov LG (2010). Available at http://www.leokrut.com/leocrystal.html.
7. The melting temperature and enthalpy of crystallization of ZnO were calculated on the basis of the *US Patent 3,043,671* "Zinc oxide crystal growth method."

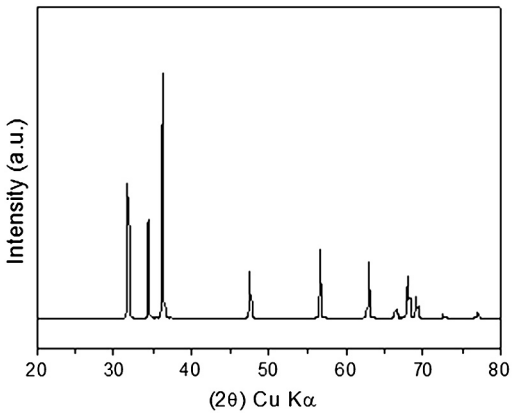

Fig. S1. Powder XRD pattern recorded on the ZnO assemblies. All the diffraction peaks in the pattern can be indexed on wurtzite ZnO (JCPDF 80-0075).

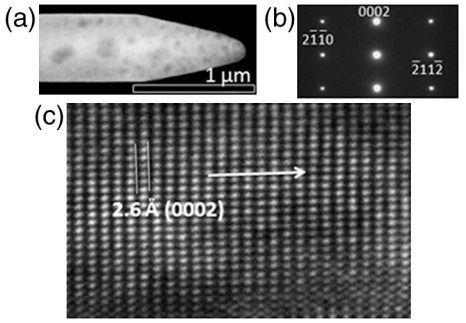

Fig. S2. (*a*) TEM image of an O-polar ZnO arm. (*b*) Selected-area electron diffraction pattern and (*c*) high-resolution TEM image.

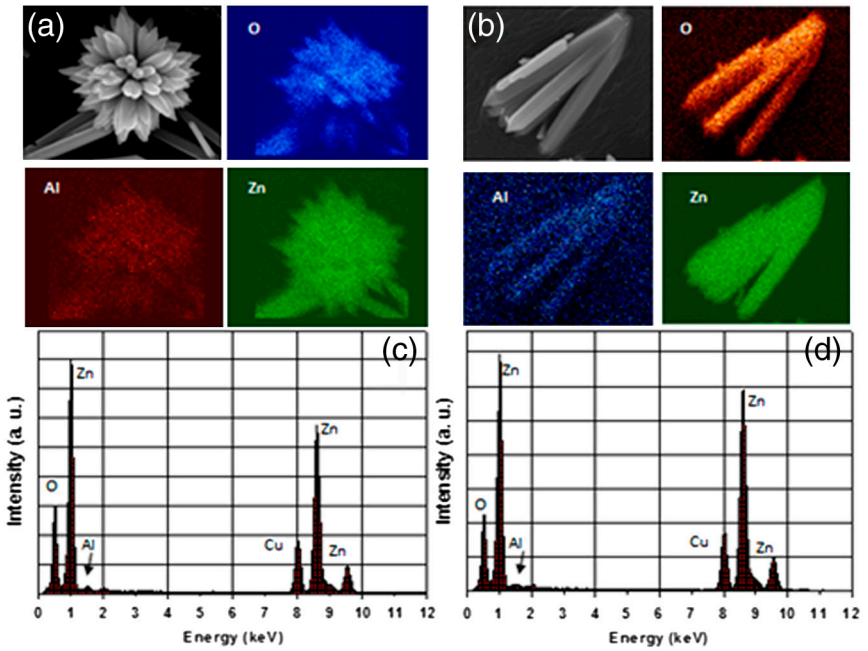

Fig. S3. (*a* and *b*) SEM and EDS mapping images of an O-polar assembly corresponding to Zn, Al, and O. (*c* and *d*) Corresponding EDS spectra of a smooth tip and a sharp tip ZnO assembly.

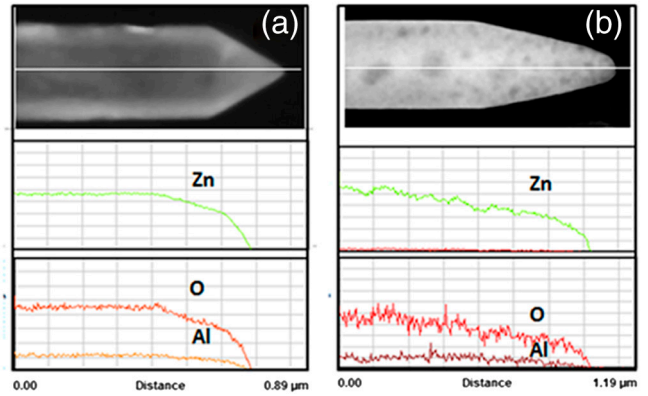

Fig. S4. TEM images of (*a*) a sharp tip and (*b*) a smooth tip ZnO arm. (*Lower*) The corresponding elemental compositions estimated from EDS mapping recorded along a white line shown in the images.

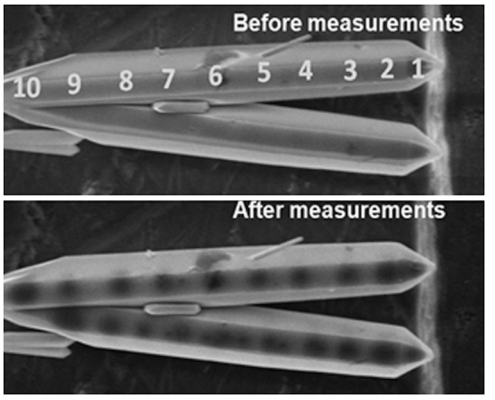

Fig. S5. SEM images of two Zn-polar ZnO rods before and after CL investigations.

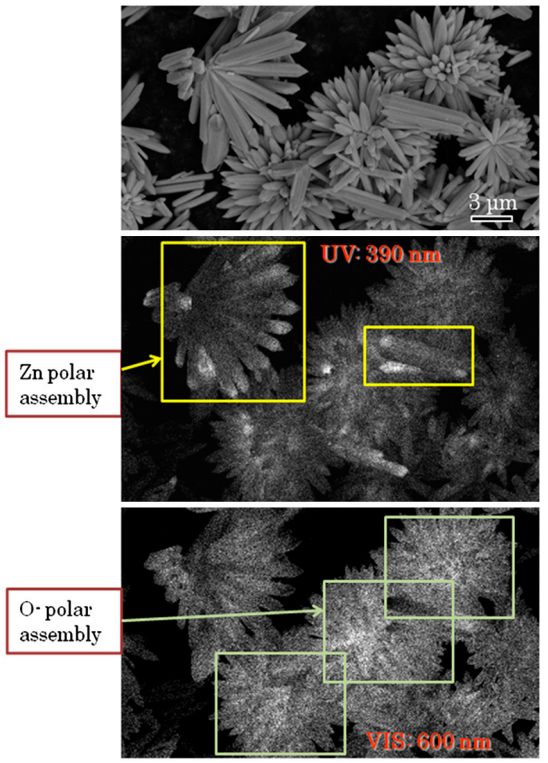

Fig. S6. Low-magnification (*a*) SEM and (*b*, *c*) CL mapping images of the assemblies. In the image, both Zn-polar and O-polar assemblies are seen together. (Image condition: accelerating voltage of 10 kV and 2,000-pA probe current).

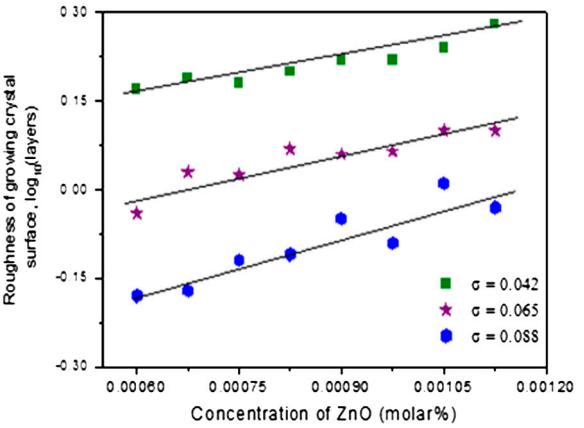

Fig. S7. Plot of surface roughness of a growing ZnO crystal calculated for various surface energies and precursor concentrations.